Applied Catalysis B: Environmental 111–112 (2012) 424–432

Contents lists available at SciVerse ScienceDirect

Applied Catalysis B: Environmental

journal homepage: www.elsevier.com/locate/apcatb

Kinetics of the $NO/H_2/O_2$ reactions on natural gas vehicle catalysts—Influence of Rh addition to Pd

Y. Renème, F. Dhainaut, P. Granger*

Unité de Catalyse et de Chimie du Solide UMR CNRS 8181, Université Lille Nord de France, Université Lille 1 Sciences et Technologies, bâtiment C3, 59650 Villeneuve d'Ascq, France

ARTICLE INFO

Article history:
Received 6 June 2011
Received in revised form 17 October 2011
Accepted 21 October 2011
Available online 25 October 2011

Keywords:
Kinetics
NO/H_2 reaction
N_2O selectivity
Pd and Rh based catalysts
Reaction mechanism
Bimetallic catalysts

ABSTRACT

This paper reports an extensive kinetic study of the NO/H_2 reaction on monometallic and bimetallic Pd and Rh based catalysts. The presence of oxygen in the feed has been examined and found to strongly alter the kinetic behaviour of noble metals according to the extent of the H_2/O_2 reaction which competes with the NO/H_2 reaction. Rate measurements have been discussed based on two different mechanisms which essentially differ from the nature of the NO dissociation step. On Pd/Al_2O_3, the predominant H_2/O_2 reaction depletes the surface hydrogen concentration inducing a dissociation step on a nearest-neighbour vacant site whereas hydrogen assists the dissociation of NO on Rh/Al_2O_3. Regarding Pd-Rh/Al_2O_3, none competitive adsorptions would likely occur with NO preferentially adsorbed on Rh. Such a result is supported by the weak partial pressure dependencies of the selectivity to N_2O formation similarly to Rh/Al_2O_3 which demonstrates that only Rh is involved in the formation of N_2 and N_2O on Pd-Rh/Al_2O_3. Nevertheless, it was found that Rh incorporation to Pd has a strong detrimental effect on the formation of nitrogen which suggests that structural might alter the adsorptive properties of rhodium in interaction with palladium.

1. Introduction

The NO/H_2 reaction has received in the past a peculiar interest mainly over rhodium based catalysts in order to understand the kinetics of this reaction on conventional three-way-catalysts (TWCs) for gasoline engine exhaust gas and ultimately to envisage the replacement of Rh that represents a cost effective solution [1,2]. The kinetics of the most representative reactions involved on TWCs, such as the NO/CO and NO/H_2 reactions, have been the subject of a wide number of publications from surface science approaches [3–7], performed under ultra-high vacuum (UHV), to more realistic conditions at atmospheric pressure [2,8–12]. From those investigations, Rh was found as the most active noble metal to dissociate NO under UHV conditions [13]. However, at the same time, its poor selective behaviour related to a predominant formation of N_2O at low temperature and low NO_x conversion, typically during the cold start engine, was pointed out. In those operating conditions, a strong NO adsorption on Rh prevents the re-adsorption of N_2O and its subsequent dissociation to nitrogen [14]. This behaviour can be considered as a serious drawback in the near future if unregulated N_2O emissions, having a much higher global warming potential than CO_2, would be accounted for in the next Euro 6 standard regulation. Up to now, most of the attempts to replace rhodium failed that actually still represents the major element in the catalytic active phases due to its intrinsic properties to dissociate NO much more readily than on the other noble metals.

Recently, the use of hydrogen for the reduction of NO_x to nitrogen received a careful attention for various reasons. First, strong efforts are now dedicated to lower fuel consumption and minimize CO_2 emissions well-recognized as greenhouse gas. Accordingly, the use of H_2 as reducing agent might be a relevant option to fulfill this specific requirement but the intermediate formation of N_2O, particularly on rhodium, must also receive a particular attention and was found to strongly depend on the nature of the reducing agent. Hence, the gain provided by hydrogen in minimizing CO_2 emissions would be compensated by greater emissions of N_2O. The second aspect to be considered in this approach is related to the emergence of novel technologies implying the set up of after-treatment systems running near stoichiometric conditions under oscillating regime, typically natural gas vehicle (NGV) catalysts [15,16], and/or the well-known lean NO_x trap/reduction system running in sequential conditions with successive exposures to lean and rich atmospheres in order to restore periodically the trap capacity and to reduce NO_x emitted to nitrogen on metallic Rh particles [17,18]. Hydrogen is more efficient than CO to restore the capacity of NO_x trap at low temperature. However, it is also well-recognized as none selective in the presence of oxygen [19]. There are also some evidences that the simultaneous removal of

* Corresponding author. Tel.: +33 3 20 43 49 38; fax: +33 3 20 43 65 61.
E-mail address: pascal.granger@univ-lille1.fr (P. Granger).

0926-3373/$ – see front matter © 2011 Elsevier B.V. All rights reserved.
doi:10.1016/j.apcatb.2011.10.030

NO_x and methane from NGV exhaust could involve H_2 even at high temperature via reforming coupled to the water–gas-shift reaction. Generally, the H_2/O_2 occurs much more readily over noble metals than the NO/H_2 reaction that may drastically lower the relevance of noble metals for those specific applications. Nevertheless, outstanding results were recently obtained on supported noble metal catalysts over reducible supports even in lean conditions showing that hydrogen can be selective even at very low temperature representing a significant breakthrough for future developments of efficient end-of-pipe technologies during the cold start engine [20–22].

This study is devoted to a better understanding of the effective role of rhodium in the NO/H_2 reaction in the presence of oxygen near stoichiometric conditions. Particular attention will be paid after rhodium addition to palladium in order to highlight the impact on the selectivity depending on the balance of the NO/H_2 and H_2/O_2 reactions but also in terms of selectivity towards the production of N_2 and N_2O. Changes in the intrinsic properties of Pd after Rh incorporation will be discussed quantitatively based on previous mechanism proposals for which the beneficial effect of hydrogen in NO dissociation has been taken into account. It will be found that changes in the nature of NO dissociation step might depend on the composition of the exhaust gas and likely on the nature of interactions between Pd and Rh.

2. Experimental

2.1. Catalyst preparation and characterization

Supported Pd and Rh-based catalysts were prepared according to a classical wet impregnation of γ-Al_2O_3 support ($250\,m^2\,g^{-1}$) with aqueous rhodium and palladium nitrate solutions to obtain ultimately 2.5 and 0.18 wt.% palladium and rhodium. Precursors were calcined in air at 500 °C for 4 h and then reduced in pure H_2 at 500 °C. H_2-temperature-programmed reduction experiments (H_2-TPR) on calcined samples were carried out on a Micromeritics Autochem II instrument under a flow of 5 vol.% H_2 diluted in Ar. H_2 chemisorption measurements were carried out at 100 °C using a pulse technique. Prior to H_2 adsorption, all the catalysts were pre-heated in pure H_2 at 500 °C and then out-gassed in flowing helium at 400 °C. Metal dispersions reported in Table 1 were calculated assuming an atomic H/M ratio equal to 1 with M = Pd, Rh or Pd-Rh. XPS experiments were performed using a Vacuum Generators Escalab 220XL spectrometer equipped with a monochromatized aluminum source for excitation in the analysis chamber under UHV conditions (~10^{-10} Torr). Binding energy (B.E.) values were referenced to the binding energy of the Al 2p core level (74.6 eV). Simulation of the experimental photopeaks was carried out using a mixed Gaussian/Lorentzian peak fit procedure according to the software supplied by VG Scientific. Semi-quantitative analysis accounted for a non-linear Shirley background subtraction [23,24].

2.2. Kinetic measurements

Steady-state catalytic measurements were performed in a recycling fixed bed flow reactor running at atmospheric pressure with a recycling ratio of 180 which created a CSTR performance. The catalytic set up was described elsewhere [25]. The gaseous mixture was analysed by a *Balzers* quadrupole mass spectrometer and a *Hewlett Packard 5890 series II* chromatograph fitted with a thermal conductivity detector. Reactants and products were separated on a *CTR1* column supplied by *Alltech*. Typically, catalytic measurements were performed with 0.1 g of catalyst, diluted with 0.2 g of α-Al_2O_3, and a global flow rate of $10\,L\,h^{-1}$. Before reaction, the catalyst samples were *in situ* reduced in hydrogen at 500 °C. The catalysts were in powder form with an average grain size of 150 μm.

Previous steady-state experiments by modifying the catalyst loading at constant space velocity did not reveal changes in the reaction rate emphasizing the absence of significant external diffusion phenomena. It was also checked that internal diffusion did not occur significantly according to the estimate of the effectiveness factor η in our experimental conditions. η was estimated based on the calculation of the Weisz modulus given by Eq. (1) corresponding to the modified criteria $\phi^2\eta$ related to none isothermal reactions and taking into account any apparent reaction order values.

$$\phi^2\eta = R^2\frac{r_{obs}\rho_p}{CD_e} \quad (1)$$

R represented the radius of the grain ~1.5×10^{-4} m, r_{obs} the experimental specific rate, ρ_p the catalyst density ($10^6\,g\,m^{-3}$), C the inlet concentration of gaseous NO ($0.05\,mol\,m^{-3}$), D_e the effective diffusion coefficient (~$10^{-6}\,m^2\,s^{-1}$) assuming a Knudsen regime [26]. The estimates for the Weisz modulus remained very low (~10^{-2}) that corresponded to numerical solutions for η very close to the unity. The occurrence of heat transfer was also evaluated on the basis of the calculation of the Prater number $\beta_1 \sim 2.6\times10^{-4}$ taking into account a thermal conductivity coefficient λ_e of approximately $0.2\,W\,m^{-1}\,K^{-1}$. Accordingly, the maximum deviation in temperature between the core and the surface of the grain should not exceed 0.1 °C in this present study [27]. Based on these calculations, it was expected that rate measurements were likely performed in chemical regime with the absence of significant heat and mass transfer phenomena.

In our operative conditions, no ammonia formation was detected and it was also checked that the successive N_2O/H_2 did not occur significantly in our experimental conditions with NO conversion lower than 15%. N_2 and N_2O were predominantly formed according to the following set of reaction.

$$2NO + 2H_2 = N_2 + 2H_2O \quad (2)$$

$$2NO + H_2 = N_2O + H_2O \quad (3)$$

Hence, the conversion of NO by reaction with H_2 (X_{NO/H_2}) was calculated according to Eq. (4) where, X_{N_2} and X_{N_2O} were respectively the conversion of NO into nitrogen and nitrous oxide. $F^0_{H_2}$ was the inlet molar flow rate of H_2, whereas, F_{N_2} and F_{N_2O} were the outlet molar flow rates of N_2 and N_2O respectively.

$$X_{NO/H_2} = \frac{2F_{N_2} + F_{N_2O}}{F^0_{H_2}} = \left(X_{N_2} + \frac{X_{N_2O}}{2}\right)\frac{F^0_{NO}}{F^0_{H_2}}, \quad (4)$$

The specific rate was calculated according to Eq. (5):

$$r_1 = \frac{F^0_{H_2}X_{NO/H_2}}{m}(mol\ h^{-1}\,g^{-1}). \quad (5)$$

m was the mass of catalyst. The N_2O selectivity (S_{N_2O}), corresponding to the transformation of NO into N_2O given by Eq. (6), was easily related to the relative rate r_{N_2}/r_{N_2O}.

$$S_{N_2O} = \frac{r_{N_2O}}{r_{N_2O} + r_{N_2}} = \frac{1}{1 + (r_{N_2}/r_{N_2O})} \quad (6)$$

r_{N_2O} and r_{N_2} were respectively the rate of NO conversion into N_2O and N_2.

3. Results

3.1. Bulk and surface characterization

As illustrated in Fig. 1, H_2-TPR profiles recorded on calcined Pd/Al_2O_3 show a fast reduction of oxidic palladium species with a maximum in H_2 uptake at 30 °C. An estimation of the atomic

Table 1
Ex situ XPS analysis of calcined supported monometallic and bimetallic Pd and Rh catalysts Pt on γ-Al_2O_3.

Catalyst	Pretreatment	B.E. (eV)[a]		Surf. XPS composition[b]			D^c
		Pd $3d_{5/2}$	Rh $3d_{5/2}$	Pd/Al	Rh/Al	Rh/Rh + Pd	
2.5Pd/Al_2O_3	Oxidative	336.6		5.6×10^{-3}			
	Reductive	335.4		4.3×10^{-3}			0.26
0.18Rh/Al_2O_3	Oxidative		310.0		2.4×10^{-3}		
	Reductive		307.1		2.2×10^{-3}		>1
2.5Pd-0.18Rh/Al_2O_3	Oxidative	336.8	309.0	8.9×10^{-3}	1.0×10^{-3}	0.10/0.16[d]	
	Reductive	335.6	306.9	6.2×10^{-3}	1.1×10^{-3}	0.15	0.31

[a] Binding energy (accuracy ±0.2 eV).
[b] Relative accuracy equal to ±20% on the atomic M/Al ratio with M = Pd or Rh.
[c] Noble metal dispersion estimated from H_2 titration on pre-reduced catalysts assuming H/M = 1.
[d] Calculated from bulk composition.

H/Pd ratio near 2.4 essentially reveals the stabilization of PdO. The slight overestimation can be ascribed to the formation of subsurface and/or bulk hydrides PdH_x as described elsewhere [28] and supported by the subsequent the production of H_2 at ∼82 °C due to their decomposition. It is noticeable that Rh incorporation does not change significantly the reducibility of PdO in the bimetallic catalyst. On the other hand, a significant attenuation of the H_2 production peak is remarkable. Extra H_2-TPR experiments were repeated on samples exposed to hydrogen at RT that revealed a complete reduction of PdO_x. In that conditions the decomposition of PdH_x can be studied isolately showing that bulk hydrides form in lower extent on 2.5Pd-0.18Rh/Al_2O_3 (22.6 vs. 39.4 μmol/g) but decomposes more readily than on Pd/Al_2O_3. XPS measurements are summarized in Table 1 with B.E. values corresponding to the Pd $3d_{5/2}$ core level representative of Pd^{2+} stabilized as PdO on calcined Pd/Al_2O_3 [29]. After *in situ* H_2 reduction, the Pd $3d_{5/2}$ photopeak shifts to lower B.E. at 335.4 eV characteristic of Pd^0. Examination of the B.E. values recorded on Rh $3d_{5/2}$ photopeaks characterizes similar trends with the presence of Rh^{3+} and then metallic rhodium species respectively on calcined and reduced samples. As indicated in Table 1, subsequent comparison relative to the Rh $3d_{5/2}$ photopeak shows a significant shift from 310.0 to 309.0 eV respectively on calcined 0.18Rh/Al_2O_3 and 2.5Pd-0.18Rh/Al_2O_3. The former value differs from those currently reported for Rh^{3+} in Rh_2O_3 (308.5 eV [30,31]) that could reflect changes in the chemical environment of Rh^{3+} with preferential interactions of isolated oxidic rhodium species with alumina [32,33] in 0.18Rh/Al_2O_3 whereas Rh^{3+} species as Rh_2O_3 would prevail in the calcined 2.5Pd-0.18Rh/Al_2O_3. On the other hand, no significant changes seems to occur on the characteristic photopeak of Rh and Pd in the reduced bimetallic sample compared with the corresponding monometallic catalysts that do not reveal strong perturbations on the electronic properties of Rh and Pd properties contrarily to earlier observations on Pd-Ag systems [34]. However, one cannot rule out local disturbance due to alloying effect that would not be sufficiently intense to provoke significant changes on the B.E. of the Pd 3d core level due to a very low Rh loading. Subsequent comparisons of the relative surface concentrations of noble metals can be achieved on the basis of the calculation of the atomic M/Al ratio. Bulk atomic Pd/Al and Rh/Al ratio are respectively equal to 4.8×10^{-3} and 0.9×10^{3}. Surface Pd and Rh concentrations on monometallic catalysts largely exceed the bulk compositions particularly on reduced 0.18Rh/Al_2O_3 which seems in relative good agreement with a high Rh dispersion on alumina calculated from by H_2 titration. This tendency is still true by comparing the surface and bulk Pd concentration on 2.5Pd-0.18Rh/Al_2O_3. On the other hand, in this latter case the atomic Rh/Al ratio tends to the bulk value irrespective to the nature of the thermal treatment that suggests possible preferential interactions between Rh and Pd rather than the segregation of well-dispersed Rh species in interaction with alumina as observed on 0.18Rh/Al_2O_3.

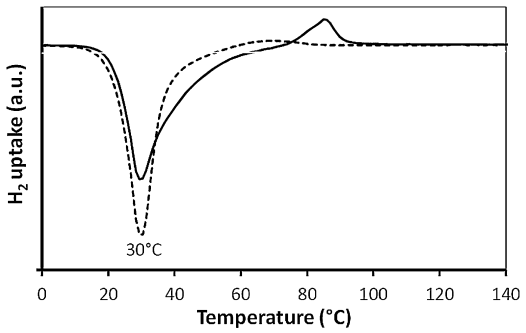

Fig. 1. H_2-temperature-programmed experiments on calcined 2.5Pd/Al_2O_3 (—) and 2.5Pd-0.18Rh/Al_2O_3 (—). Experimental conditions: 5 vol.% H_2 diluted in Ar with $dT/dt = 5\,°C\,min^{-1}$.

3.2. Comparative theoretical and experimental kinetic approaches of the NO/H_2 reaction

3.2.1. Preliminary theoretical calculations based on the unity bond index-quadratic exponential potential (UBI-QEP) method

This mathematical method has been earlier develop by Shustorovich et al. [35–37] providing straightforwardly heat of adsorption for molecular and atomic chemisorbed species and activation energies for elementary reactions. Previous calculations were performed on model Pd(1 1 1) and Pt(1 1 1) surfaces for DeNO$_x$ reactions considering a panel of elementary steps earlier suggested for explaining the formation of N_2 and N_2O [38]. In this study, we have extended those calculations on Rh(1 1 1).

Among the different mechanism proposals, the formation of N_2 can be currently explained by the associative desorption of two adjacent chemisorbed N atoms or involving interactions between N_{ads} and NO_{ads} as described in Fig. 2. Let us note that this latter step can be also suggested for depicting the formation of N_2O as previously demonstrated from surface science under UHV and also at higher pressure conditions on Rh(1 1 1) [6,7,12] equally with a bimolecular reaction between two adjacent adsorbed NO molecules as earlier envisioned by Burch and Coleman [9] who suggested this reaction pathway for the production of N_2O on supported Pt catalysts at low temperature. The assistance of H_{ads} in the dissociation of NO_{ads} as described in step (10) for the NO/H_2 reaction has been envisioned, whereas Mechanism 1.b accounts for a dissociation step of NO_{ads} on a nearest-neighbour vacant site. Those calculations account for NO coordinated via the N atom to a two-fold bridge site and consider adsorption at zero coverage which corresponds to a boarder case far from our experimental conditions at atmospheric pressure. Taking into account those realistic conditions corresponding to high coverage with possible lateral repulsive interactions and a more

Mechanism 1.a

(7) $NO + * \leftrightarrows NO_{ads}$
(8) $H_2 + 2* \leftrightarrows 2\ H_{ads}$
(9) $O_2 + 2* \leftrightarrows 2\ O_{ads}$
(10) $NO_{ads} + H_{ads} \rightarrow N_{ads} + OH_{ads}$
(11) $N_{ads} + N_{ads} \rightarrow N_2 + 2*$
(12) $NO_{ads} + N_{ads} \rightarrow N_2 + O_{ads} + *$
(13) $NO_{ads} + N_{ads} \rightarrow N_2O + 2*$
(14) $O_{ads} + H_{ads} \rightarrow OH_{ads} + *$
(15) $OH_{ads} + H_{ads} \rightarrow H_2O + 2*$

Mechanism 1.b

(7) $NO + * \leftrightarrows NO_{ads}$
(8) $H_2 + 2* \leftrightarrows 2\ H_{ads}$
(9) $O_2 + 2* \leftrightarrows 2\ O_{ads}$
(10') $NO_{ads} + * \rightarrow N_{ads} + O_{ads}$
(11) $N_{ads} + N_{ads} \rightarrow N_2 + 2*$
(12) $NO_{ads} + N_{ads} \rightarrow N_2 + O_{ads} + *$
(13) $NO_{ads} + N_{ads} \rightarrow N_2O + 2*$
(14) $O_{ads} + H_{ads} \rightarrow OH_{ads} + *$
(15) $OH_{ads} + H_{ads} \rightarrow H_2O + 2*$

Fig. 2. Mechanism schemes earlier proposed for the NO/H_2 reaction over noble metals [1,6].

representative on-top NO coordination, a lower heat of adsorption can be expected [35]. Kinetic and thermodynamic parameters calculated in Table 2 on Rh(1 1 1) are compared with those earlier estimated on Pd(1 1 1) [38]. This comparison shows that similarly to Pd(1 1 1), NO adsorbs more strongly than H_2 on Rh(1 1 1). But the most important feature is related to the greatest numerical values for the heat of oxygen adsorption both on Pd(1 1 1) and Rh(1 1 1) which suggests that the surface could be quasi-completely covered by O_{ads} depending on the partial pressure and temperature conditions selected for the NO/H_2 reaction. These findings agree with previous surface science studies on model catalysts with lower activation barriers associated with steps for the dissociation of NO on Rh(1 1 1). Similarly to Pd(1 1 1), it is also worthwhile to mention that the promotional effect of H_{ads} in NO dissociation to N_{ads} and OH_{ads} leads to a lessening of the activation energy on Rh(1 1 1). Let us note that a significant decrease in the activation energy for the associative desorption of nitrogen on Rh(1 1 1) in comparison to Pd(1 1 1) combined to a greater extent of NO dissociation can originate further enhancements in nitrogen production on rhodium. However, under typical atmospheric conditions the predominance of N_2O formation earlier evidenced at low temperature [39,40], typically when Rh is quasi-completely covered by strongly chemisorbed NO molecules, could be explained by the occurrence of elementary steps involving bimolecular reactions between two chemisorbed NO molecules characterized by a low activation barrier and/or alternately between NO_{ads} and N_{ads} in accordance with references [6,7,12,9] (see Fig. 2).

3.2.2. Steady-state kinetic measurements on mono- and bimetallic Pd and Rh based catalysts

Steady state rate measurements were performed on pre-reduced catalysts in H_2 at 500 °C under stoichiometric conditions with inlet partial pressures of NO, H_2 and O_2 of respectively 9.5×10^{-4}, 3.0×10^{-3} and 1.0×10^{-3} atm in the temperature range 30–210 °C. As seen in Table 3, significant changes in the apparent activation energy values are distinguishable mainly on $0.18Rh/Al_2O_3$ exhibiting the lowest value calculated from the slope of the Arrhenius plots (see Fig. 3). Such a decrease in the apparent activation energy may have several explanations related to the peculiar adsorptive properties on Rh and Pd but also to possible change in the nature of the dissociation step of NO according to activation barrier calculated in Table 2. As seen an intermediate value characterizes $2.5Pd\text{-}0.18Rh/Al_2O_3$ between those measured on the corresponding monometallic catalysts.

Regarding rate calculations in Table 3, subsequent comparisons can only be achieved on $2.5Pd/Al_2O_3$ and $2.5Pd\text{-}0.18Rh/Al_2O_3$ with specific rates recorded at the same temperature of 40 °C. On the other hand, $0.18Rh/Al_2O_3$ exhibits an unexpectedly poor specific activity at much higher temperature of 210 °C. Such a trend agrees with previous observations on supported Rh catalysts on NaX and alumina that report strong differences according to the nature of the reducing agent [39,40]. Hence, in the presence of CO, Rh is usually the most active according to the following sequence $Rh \gg Pd \cong Pt$ whereas the opposite behaviour takes place in the presence of hydrogen $Pt \gg Pd > Rh$ where Rh is less active in that case. As explained, NO adsorption would hinder the dissociation of hydrogen which results in the lowest activity and an intermediate formation of N_2O. As observed, Rh addition to Pd has no significant influence on the rate of the NO/H_2 reaction with comparable values

Table 2
Enthalpies (ΔH) and activation energies (E) in kJ mol^{-1} of suggested elementary steps for the NO/H_2 reaction on Pd(1 1 1) and Rh(1 1 1) from UBI-QEP calculations.

Reaction	Rh(1 1 1)		Pd(1 1 1)[a]	
	ΔH	E	ΔH	E
$NO_g + * \rightarrow NO_{ads}$	−109	0	−134	0
$H_{2\,g} + 2* \rightarrow 2H_{ads}$	−76	12	−84	9
$O_{2\,g} + 2* \rightarrow 2O_{ads}$	−357	0	−232	0
$NO_{ads} + * \rightarrow N_{ads} + O_{ads}$	−172	27	−143	38
$NO_{ads} + H_{ads} \rightarrow N_{ads} + OH_{ads}$	−130	9	−113	7
$NO_{ads} + H_{ads} \rightarrow NH_{ads} + O_{ads}$	−40	39	1	89
$N_{ads} + N_{ads} \rightarrow N_{2g} + 2*$	27	112	142	179
$NO_{ads} + N_{ads} \rightarrow N_{2g} + O_{ads} + *$	−145	0	−1	53
$NO_{ads} + N_{ads} \rightarrow N_2O_g + 2*$	114	114	197	197
$NO_{ads} + NO_{ads} \rightarrow N_2O_g + O_{ads} + *$	−58	0	53	60
$O_{ads} + H_{ads} \rightarrow OH_{ads} + *$	42	101	30	91
$OH_{ads} + H_{ads} \rightarrow H_2O_g + 2*$	−24	52	−67	0

[a] See reference [38].

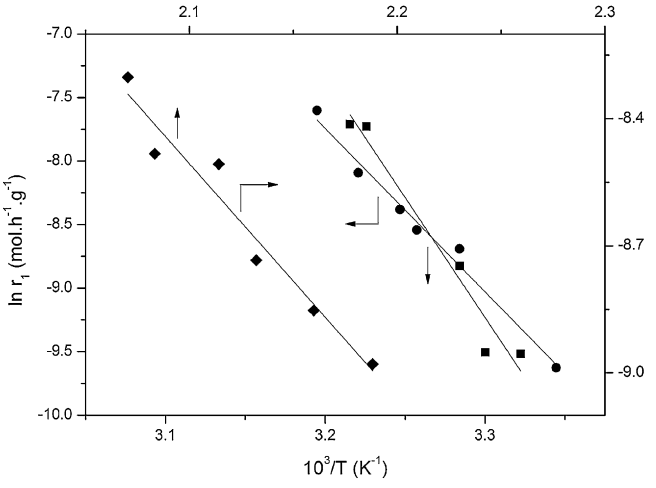

Fig. 3. Arrhenius plots for the NO/H_2 reaction under stoichiometric conditions with inlet pressure of NO, H_2 and O_2 of respectively 9.5×10^{-4}, 3.0×10^{-3} and 1.0×10^{-3} atm in the temperature range 30–210 °C on pre-reduced $2.5Pd/Al_2O_3$ (■); $0.18Rh/Al_2O_3$ (♦); $2.5Pd\text{-}0.18Rh/Al_2O_3$ (●).

Table 3
Steady state rates and kinetic parameters calculated on pre-reduced monometallic and bimetallic Pd and Rh based catalysts in pure H_2 at 500 °C for the competitive NO/H_2 and H_2/O_2 reactions.

Catalysts	D (%)	T (°C)	E_{app} [b] (kJ mol^{-1})	r_1 (NO/H_2)[a]	r_2 (H_2/O_2)[a]	r_2/r_1	r_1' [b]
2.5Pd/Al_2O_3	26	40	156.8	2.4×10^{-4}	2.2×10^{-3}	9.2	3.9
0.18Rh/Al_2O_3	>1	210	40.4	2.0×10^{-4}	3.0×10^{-4}	1.5	11.4
2.5Pd-0.18Rh/Al_2O_3	31	40	106.8	1.9×10^{-4}	3.4×10^{-4}	1.8	4.3

[a] Specific rate expressed in mol h^{-1} g^{-1} with inlet partial pressure of NO, H_2 and O_2 of respectively 9.5×10^{-4}, 3.0×10^{-3} and 1.0×10^{-3} atm
[b] Intrinsic rate expressed in mol s^{-1} at$_{surf}^{-1}$.

on 2.5Pd/Al_2O_3 and 2.5Pd-0.18Rh/Al_2O_3 varying within the margin of error. On the other hand, the H_2/O_2 reaction is strongly affected with rate values on 2.5Pd-0.18Rh/Al_2O_3 one order of magnitude lower than those recorded on 2.5Pd/Al_2O_3. Hence, such a comparison shows in our case that a high H_2/O_2 reaction capable to liberate available vacant sites for the NO dissociation does not promote the reduction of NO/H_2 reaction on 2.5Pd/Al_2O_3.

Returning to changes observed on the rate of the H_2/O_2 at relatively low temperature ~40 °C the competition between the relative rates of palladium hydride formation/desorption processes and that of the surface oxidation reaction [41,42] could partly explain the loss of activity after Rh incorporation. The relative rate of diffusion step involved in such processes are currently related to structural considerations with the presence of surface defects and changes in the local geometrical structure around the absorption path. Rh incorporation would possibly change the local structure according to lower amount of H_2 produced from the decomposition of palladium hydrides as shown from H_2-TPR experiments. At the same time, the back diffusion of dissolved hydrogen to the surface occurring at lower temperature on 2.5Pd-0.18Rh/Al_2O_3 could retain a sufficiently high surface concentration of chemisorbed hydrogen that could preserve the H_2/O_2 reaction in contradiction with experimental evidences. Hence, the loss of activity recorded on 2.5Pd-0.18Rh/Al_2O_3 for the H_2/O_2 reaction could be rationalized if the chemisorption of oxygen is hindered after Rh incorporation.

Particular attention was paid to the NO/H_2 reaction. Steady-state rate measurements were performed under isothermal conditions but at different temperatures to obtain low conversion levels. Hence, the partial pressure dependencies of NO, H_2 and O_2 of the reaction rate r_1 were investigated at 40 °C on 2.5Pd/Al_2O_3 and 2.5Pd-0.18Rh/Al_2O_3 and 210 °C on 0.18Rh/Al_2O_3 with inlet partial pressures of NO, H_2 and O_2 varying in the range $(0.7–1.2) \times 10^{-3}$ atm, $(2.0–4.0) \times 10^{-3}$ atm and $(0.5–1.5) \times 10^{-3}$ atm respectively. The selectivity to the production of N_2O on 2.5Pd/Al_2O_3 strongly depends on the operating conditions notably on the partial pressure of NO. This observation earlier discussed can be explained by the involvement of different steps for the production of N_2 and N_2O [40]. Such behaviour differs from that characterizing 0.18Rh/Al_2O_3 because the relative rate of N_2O formation on Rh is usually insensitive to changes in NO partial pressure [12,40]. It is worthwhile to note that Rh incorporation to 2.5Pd/Al_2O_3 completely modifies the selectivity also becoming insensitive to partial pressure conditions and then mimicking the behaviour of Rh. Such peculiar behaviour is illustrated in Fig. 4 which reports the plots of r_{N_2}/r_{N_2O} vs. $\sqrt{p_{H_2}}/p_{NO}$. As seen, r_{N_2}/r_{N_2O} values on 0.18Rh/Al_2O_3 and 2.5Pd-0.18Rh/Al_2O_3 remain unchanged according to the margin of error within the NO partial pressure range contrarily to 2.5Pd/Al_2O_3. Now regarding the extrapolated values for r_{N_2}/r_{N_2O} of 1.40–1.45 on 2.5Pd-0.18Rh/Al_2O_3 at 40 °C, it is worthwhile to note that r_{N_2}/r_{N_2O} is usually higher on 2.5Pd/Al_2O_3 showing that Rh incorporation has a detrimental effect of the production of nitrogen in the bimetallic catalyst.

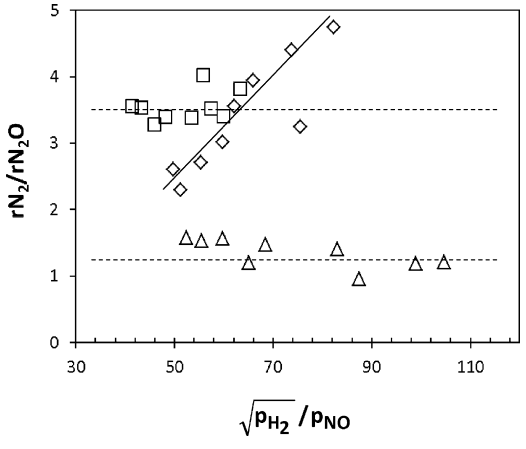

Fig. 4. Selectivity behaviour of 2.5Pd/Al_2O_3 (◊); 0.18Rh/Al_2O_3 (□); 2.5Pd-0.18Rh/Al_2O_3 (△) reflected by changes in the relative rate r_{N_2}/r_{N_2O} vs. $\sqrt{p_{H_2}}/p_{NO}$ under steady-state conditions according to the following conditions with constant inlet partial pressures of H_2 and O_2 of respectively 3.0×10^{-3} and 1.0×10^{-3} atm and NO partial pressure varying in the range $(0.7–1.2) \times 10^{-3}$ atm.

4. Discussion

As observed in our operating conditions only N_2 and N_2O were detected that emphasizes the fact that the formation of ammonia previously characterized in reductive atmosphere is suppressed probably because of the competitive H_2/O_2 reaction that depletes the hydrogen coverage when oxygen is added in the feed even near stoichiometric conditions. It is remarkable that this kinetic feature is more accentuated on 2.5Pd/Al_2O_3. It was also found that no formation of NO_2 is observed in the temperature range of the study irrespective of the catalysts composition.

Theoretical calculations initiated by Shustorovich et al. [35–37] by developing the bond order conservation Morse potential and further its generalization as the Unity Bond Index-Quadratic exponential Potential (UBI-QEP) has been extended in this present study to Rh(1 1 1) leading to comparable trends than those earlier established on Pd(1 1 1) (see Table 2) which suggest that hydrogen might play a key role in determining the extent of NO dissociation as illustrated in Mechanism 1.a. However, the situation could be different in this study because of the predominant H_2/O_2 reaction in the presence of oxygen, particularly on 2.5Pd/Al_2O_3, that induces low residual H coverage. Frank et al. [8] modeled the NO/H_2/O_2 reaction on the basis of Mechanism 1.b on Pt-Mo-Co/α-Al_2O_3 in the temperature range 142–160 °C involving NO dissociation on a nearest neighbour vacant site that can be liberated when O_{ads} reacts more promptly with H_{ads}. Consequently, the probability for findings NO_{ads} at the vicinity of H_{ads} has been considered in that case as very poor. Subsequent optimization of the heat of H_2, NO and O_2 adsorption from rate measurements of respectively −59, −77 and −97 kJ mol^{-1} are substantially greater than the theoretical values derived from the UBI-QEP theory respectively equal to −75, −109 and −213 kJ mol^{-1} [39]. However, it is noticeable that both series emphasize the fact the O_2 adsorption would likely predominate over noble metals even at moderate oxygen concentrations.

4.1. Reaction mechanisms and calculations of kinetic and thermodynamic constants for adsorption

4.1.1. On monometallic catalysts

As found, monometallic Pd catalyst is much more active than Rh which is quite unexpected because previous surface science investigations found that NO dissociation occurs more readily on Rh than on Pd. Even if the activation barrier for the NO/H_2 is lower on Rh/Al_2O_3, such a former comparison could be related to the very high dispersion of Rh with possible segregation of isolated Rh^{3+} species. Such an explanation is partly supported by *in situ* XPS measurements on reduced samples with a high surface metallic Rh concentration in agreement with H_2 titration indicating a high Rh dispersion. Such a configuration would not be optimal according to previous surface science investigations [43] which showed that a complicate structure composed of several atoms is needed with a specific arrangement for obtaining a set of surface orbitals conductive for the reaction. Hence, the poorest activity of Rh/Al_2O_3 could be related to a possible loss of its metallic character in reaction conditions in the presence of oxygen and/or to small Rh clusters with morphology that do not promote the structure sensitive NO dissociation step. In fact, the stabilization of less reactive nitrosyl species seems in line with previous explanations showing that NO would prevent the adsorption of hydrogen on Rh [39].

A rate equation previously established [38] can be derived from mechanisms 1.a and 1.b which accounts for the following set of assumptions: (i) NO dissociation step as rate determining, (ii) fast adsorptions of the reactants at equilibrium, and (iii) chemisorbed H and O atoms and NO molecules as the most abundant species at the surface. For Mechanism 1.a involving a dissociation of NO assisted by H_{ads} the rate expression is given by Eq. (16), whereas Eq. (17) corresponds to Mechanism 1.b involving a nearest-neighbour vacant site for the dissociation of NO.

$$r_{1.a} \cong k_{10}\theta_{NO}\theta_H = \frac{k_{10}K_{NO}P_{NO}\sqrt{K_{H_2}P_{H_2}}}{\left(1 + K_{NO}P_{NO} + \sqrt{K_{H_2}P_{H_2}} + \sqrt{K_{O_2}P_{O_2}}\right)^2}, \quad (16)$$

$$\text{or } r_{1.b} \cong k_{10'}\theta_{NO}\theta_V = \frac{k_{10'}K_{NO}P_{NO}}{\left(1 + K_{NO}P_{NO} + \sqrt{K_{H_2}P_{H_2}} + \sqrt{K_{O_2}P_{O_2}}\right)^2} \quad (17)$$

$$\text{with } \theta_{NO} = \frac{K_{NO}P_{NO}}{1 + K_{NO}P_{NO} + \sqrt{K_{H_2}P_{H_2}} + \sqrt{K_{O_2}P_{O_2}}}, \quad (18)$$

$$\theta_H = \frac{\sqrt{K_{H_2}P_{H_2}}}{1 + K_{NO}P_{NO} + \sqrt{K_{H_2}P_{H_2}} + \sqrt{K_{O_2}P_{O_2}}} \quad (19)$$

$$\text{and } \theta_V = \frac{1}{1 + K_{NO}P_{NO} + \sqrt{K_{H_2}P_{H_2}} + \sqrt{K_{O_2}P_{O_2}}}. \quad (20)$$

k_n and K_i are respectively the rate constant associated to step (n) and the equilibrium adsorption constant of the reactant i (i = NO, O_2 or H_2). θ_j stands for the coverage for the adsorbate j (j = NO_{ads}, H_{ads}) while θ_v corresponds to the fraction of vacant sites.

As above-mentioned, it seems obvious that the nature of steps for NO dissociation could be strongly altered by the presence of oxygen. Hence, it is expected that the reaction conditions but also the surface composition of the catalysts are predominant parameters in determining the probability of mechanisms 1.a and 1.b associated with the derived rate Eqs. (16) and (17). In a first approach, we have equally considered both rate equations for the calculation of those unknown parameters. As reported elsewhere [25], the values of those kinetic and thermodynamic constants were calculated by a statistical method based on the minimization of the square difference between experimental and predicted rates according to Eq. (21). The results of the adjustment routine are summarized in Table 4 with optimized parameters providing a good correlation between predicted and experimental rates as illustrated in Fig. 5.

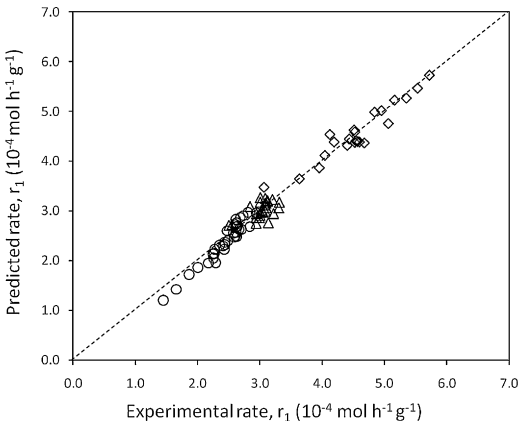

Fig. 5. Correlation between experimental and predicted rates for the NO/H_2 reaction on $2.5Pd/Al_2O_3$ (◊); $0.18Rh/Al_2O_3$ (○); $2.5Pd\text{-}0.18Rh/Al_2O_3$ (△).

$$r_1 = r_{1.a} + r_{1.b} = \frac{k_{10}K_{NO}P_{NO}\sqrt{K_{H_2}P_{H_2}}}{\left(1 + K_{NO}P_{NO} + \sqrt{K_{H_2}P_{H_2}} + \sqrt{K_{O_2}P_{O_2}}\right)^2} + \frac{k_{10'}K_{NO}P_{NO}}{\left(1 + K_{NO}P_{NO} + \sqrt{K_{H_2}P_{H_2}} + \sqrt{K_{O_2}P_{O_2}}\right)^2} \quad (21)$$

First, the adjusted values for the rate constants k_{10} and $k_{10'}$ on $2.5Pd/Al_2O_3$ are of the same order of magnitude. As seen in Fig. 6, the related contribution of $r_{1.a}$ on the overall rate r_1, of approximately 33%, indicates that both mechanisms depicted in Fig. 1 coexist with a predominant participation of Mechanism 1.b involving a dissociation step of NO on a nearest neighbour vacant site on $2.5Pd/Al_2O_3$. Such a conclusion can be related to the simultaneous H_2/O_2 reaction that occurs more readily than the NO/H_2 on $2.5Pd/Al_2O_3$. The calculated rate r_2/r_1 ratio in Table 2 and the optimized value for K_O on $2.5Pd/Al_2O_3$ significantly higher than K_H and K_{NO} seems to support this conclusion. In addition, the low value for K_{NO} signifies that the probability to find a vacant site rather than H_{ads} is much higher. Now, regarding, $0.18Rh/Al_2O_3$, the rate constant $k_{10'}$ almost nil indicates that Mechanism 1.a would likely occur. Such a conclusion is in relative good agreement with a high

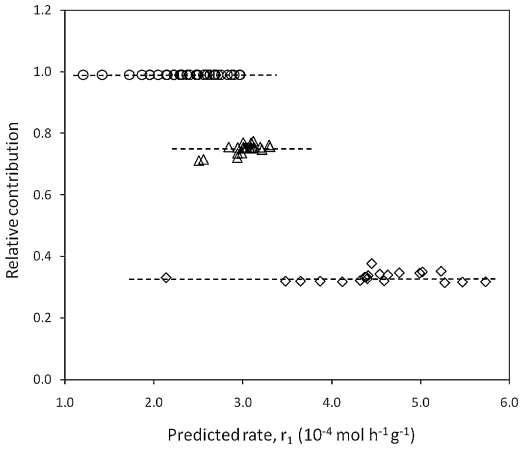

Fig. 6. Relative contribution of Mechanism 1.a involving step 10 ($NO_{ads} + H_{ads} \rightarrow N_{ads} + OH_{ads}$) with respect to Mechanism 1.b involving step 10′ ($NO_{ads} + {}^* \rightarrow N_{ads} + O_{ads}$) for the NO/H_2 reaction on $2.5Pd/Al_2O_3$ (◊); $0.18Rh/Al_2O_3$ (○); $2.5Pd\text{-}0.18Rh/Al_2O_3$ (△). NO/H_2 reaction under stoichiometric conditions with inlet pressure of NO, H_2 and O_2 of respectively 9.5×10^{-4}, 3.0×10^{-3} and 1.0×10^{-3} atm in the temperature range 30–210 °C.

Table 4
Optimized kinetic and thermodynamic parameters calculated for the NO/H_2 reaction on supported Pd and Rh based catalysts.

Catalyst	T (reaction) (°C)	k_{10} [a]	$k_{10'}$ [a]	K_{NO} (atm^{-1})	K_{H_2} (atm^{-1})	K_{O_2} (atm^{-1})
$2.5Pd/Al_2O_3$	40	0.53	0.25	4	25	200
$0.18Rh/Al_2O_3$	210	8.5×10^{-3}	≅0	700	15	75
$2.5Pd\text{-}0.18Rh/Al_2O_3$	40	5.3×10^{-3}	5.8×10^{-4}	1500	20	93

[a] mol h^{-1} g^{-1}.

value for the equilibrium adsorption constant K_{NO} much higher than the optimized value for K_O and K_H which indicates that Rh sites would be predominantly covered by NO. Regarding the lowest values calculated for the rate r_2/r_1 ratio, they suggest that the probability for finding H_{ads} at the vicinity of NO_{ads} on $0.18Rh/Al_2O_3$ would become more important.

4.1.2. On bimetallic 2.5Pd-0.18Rh/Al_2O_3

Now regarding bimetallic catalysts, two borderline cases can be envisioned which account for the preservation of the intrinsic adsorptive properties of the metals in the bimetallic particles or, alternately, the generation of electronic modifications when Rh strongly interacts with Pd leading to an overall change of the individual adsorptive properties of Pd and Rh. In this latter case averaged electronic properties can be assumed which would suggest that a bimetallic catalyst would behave like a monometallic one with the occurrence of competitive adsorptions of the reactants on a single site composed of Rh and Pd [40]. As previously found by Hu et al. [44], such electronic changes might produce synergy effects on the catalytic activity that is not observed on $2.5Pd\text{-}0.18Rh/Al_2O_3$ for the NO/H_2 reaction. In the former case none competitive adsorptions would occur. Such a scenario has been already verified for the NO/CO reaction on Pt-Rh/Al_2O_3 with preferential adsorption of NO on Rh whereas CO adsorbs on Pt [38]. Earlier investigations also found that Pt and Rh in $Pt_{10}Rh_{90}(1\,1\,1)$ preserve their individual adsorptive properties suggesting that the loss of catalytic activity in comparison with Rh(1 1 1) was essentially due to a dilution effect of Pt [45].

In a first attempt, competitive adsorptions have been examined with adjusted values for kinetic and thermodynamic constants using Eq. (21) reported in Table 4. However, further comparisons on monometallic rhodium and palladium based catalysts show that K_{NO} is substantially higher on Rh than on Pd (700 atm^{-1} on $0.18Rh/Al_2O_3$ at 210 °C vs. 4 atm^{-1} on $2.5Pd/Al_2O_3$ at 40 °C) which means that the corresponding value on Rh at 40 °C is expected to be much higher in agreement with the exothermicity of adsorption

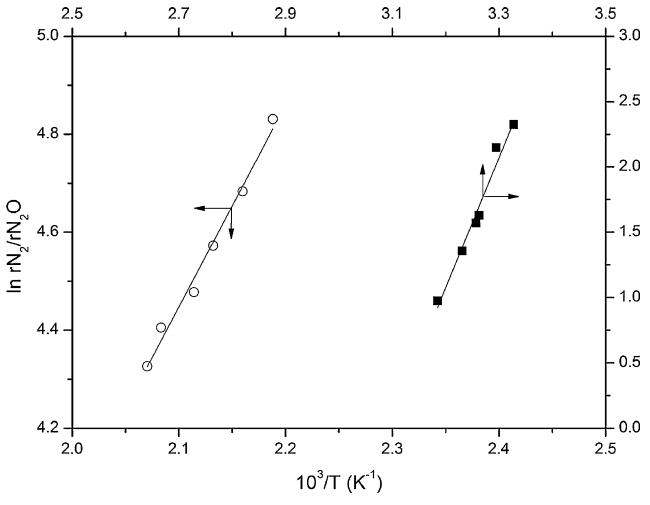

Fig. 7. Plot on $\ln r_{N_2}/r_{N_2O}$ vs. $1/T$ on $0.18Rh/Al_2O_3$ (○) and on $2.5Pd\text{-}0.18Rh/Al_2O_3$ (■).

steps. Hence, if Rh preserves its intrinsic adsorptive properties in $2.5Pd\text{-}0.18Rh/Al_2O_3$ then NO would adsorb preferentially on Rh. Subsequent comparison of the numerical values for K_H and K_O with K_{NO} on $2.5Pd/Al_2O_3$ leads to the assumption that O_2 and H_2 would preferentially adsorb on Pd. Based on these considerations, Eqs. (22)–(24) can be proposed where *′ and * stand for respectively Rh and Pd sites.

$$NO + *' \leftrightarrows NO_{ads} \quad (22)$$

$$H_2 + 2* \leftrightarrows 2H_{ads} \quad (23)$$

$$O_2 + 2* \leftrightarrows 2O_{ads} \quad (24)$$

The involvement of none competitive adsorptions of NO on Rh on bimetallic sites opens the discussion on the nature of the vacant sites at the vicinity of NO_{ads} which can be only composed of Rh, Pd or equally Rh and Pd. According to those different configurations, various complex scenarios can be envisioned by considering a mixed kinetic model of $2.5Pd\text{-}0.18Rh/Al_2O_3$ which would still account for the assistance of hydrogen in the dissociation step of NO_{ads} and also on nearest neighbour vacant sites as previously described on $2.5Pd/Al_2O_3$. Accordingly, we have examined the involvement of the following set of dissociation steps:

$$NO_{ads} + H_{ads} \rightarrow N_{ads} + OH_{ads} \quad (25)$$

$$NO_{ads} + * \rightarrow N_{ads} + O_{ads} \quad (25')$$

$$NO_{ads} + *' \rightarrow N_{ads} + O_{ads} \quad (26)$$

Based on Eqs. (25)–(26), the following rate equations can be established using the same above-mentioned set of assumptions.

$$r_1 = k_{25}\theta_{NO}\theta_H = \frac{k_{25}K_{NO}P_{NO}\sqrt{K_{H_2}P_{H_2}}}{(1+K_{NO}P_{NO})\left(1+\sqrt{K_{H_2}P_{H_2}}+\sqrt{K_{O_2}P_{O_2}}\right)}, \quad (27)$$

according to step (25),

$$r_1 = k_{25'}\theta_{NO}\theta_V = \frac{k_{25'}K_{NO}P_{NO}}{(1+K_{NO}P_{NO})\left(1+\sqrt{K_{H_2}P_{H_2}}+\sqrt{K_{O_2}P_{O_2}}\right)}, \quad (28)$$

according to step (25′) and

$$r_1 = k_{26}\theta_{NO}\theta'_V\frac{k_{26}K_{NO}P_{NO}}{(1+K_{NO}P_{NO})^2}, \quad (29)$$

according to step (26).

Examination of the partial pressure dependencies of the rate on $2.5Pd\text{-}018Rh/Al_2O_3$ showed an inhibiting effect of oxygen (result not shown) which disagree with Eq. (29) that only fit with an apparent order with respect to the oxygen partial pressure almost nil. Hence, subsequent comparisons between predicted and experimental rates were achieved by using Eq. (30).

$$r_1 = \frac{k_{25}K_{NO}P_{NO}\sqrt{K_{H_2}P_{H_2}}}{(1+K_{NO}P_{NO})\left(1+\sqrt{K_{H_2}P_{H_2}}+\sqrt{K_{O_2}P_{O_2}}\right)} + \frac{k_{25'}K_{NO}P_{NO}}{(1+K_{NO}P_{NO})\left(1+\sqrt{K_{H_2}P_{H_2}}+\sqrt{K_{O_2}P_{O_2}}\right)} \quad (30)$$

Table 5
Optimized kinetic and thermodynamic parameters calculated for the NO/H_2 reaction on $2.5Pd\text{-}0.18Rh/Al_2O_3$ according to competitive and none competitive adsorptions of the reactants.

Adsorption model	k_{10}[a]	$k_{10'}$ [a]	k_{25}[a]	$k_{25'}$ [a]	K_{NO} (atm^{-1})	K_{H_2} (atm^{-1})	K_{O_2} (atm^{-1})
Competitive	5.3×10^{-3}	5.8×10^{-4}			1500	20	93
None Competitive			1.7×10^{-3}	1.9×10^{-4}	2500	40	149

[a] $mol\,h^{-1}\,g^{-1}$.

The adjusted values in Table 5 suggest that none competitive adsorptions can also fit correctly rate measurements leading to a higher value for K_{NO} on $2.5Pd\text{-}0.18Rh/Al_2O_3$ as expected. Also, it is remarkable that the adjusted value for K_O on $2.5Pd\text{-}0.18Rh/Al_2O_3$ converges to that calculated on $2.5Pd/Al_2O_3$ which partly corroborates the set of assumptions with a preferential oxygen adsorption on Pd in the bimetallic catalyst. As shown in Fig. 5, this seems in agreement with the predominant participation of Mechanism 1.a more representative of the Rh behaviour than that of Pd. This could be also in line with a back desorption of dissolved hydrogen taking place more readily on $2.5Pd\text{-}0.18Rh/Al_2O_3$ and then preserving a higher hydrogen coverage than on $2.5Pd/Al_2O_3$. However, the participation of Mechanism 1.b cannot be neglected as well as possible competitive adsorptions on $2.5Pd\text{-}018Rh/Al_2O_3$ cannot be completely ruled out.

4.2. Discussion on the nature on elementary steps for the production of nitrogen

Subsequent examination of the selectivity towards the production of N_2 and N_2O provides more decisive arguments to state on the more likely mechanism scheme for the NO/H_2 reaction on $2.5Pd\text{-}0.18Rh/Al_2O_3$.

As earlier demonstrated S_{N_2O} depends on the relative rate r_{N_2}/r_{N_2O}. The examination of Fig. 4 shows different selectivity behaviours with unchanged relative r_{N_2}/r_{N_2O} rates on $0.18Rh/Al_2O_3$ and on $2.5Pd\text{-}0.18Rh/Al_2O_3$ when the partial pressure of NO varies. On the other hand significant changes are observable on $2.5Pd/Al_2O_3$. Such a comparison shows that, after Rh incorporation, the bimetallic catalyst mimics the behaviour of Rh only catalyst which suggests that the steps for N_2 and N_2O predominantly involves Rh in $2.5Pd\text{-}0.18Rh/Al_2O_3$. This is a strong argument in favour of none competitive adsorptions with predominant NO adsorption on Rh. As a matter of fact, such selectivity behaviour can be easily explained from steps related to N_2 and N_2O as described in Fig. 1. r_{N_2}/r_{N_2O} can be calculated as a function of θ_j and k_n related to step for the formation of N_2 and N_2O.

$$\frac{r_{N_2}}{r_{N_2O}} = \frac{k_{11}}{k_{13}}\frac{\theta_N}{\theta_{NO}} + \frac{k_{12}}{k_{13}} \tag{31}$$

θ_N/θ_{NO} can be obtained by applying the steady-state approximation to chemisorbed N atoms according to Eq. (32).

$$\frac{d\theta_N}{dt} = 0 = k_{10}\theta_{NO}\theta_H - 2k_{11}\theta_N^2 - (k_{12}+k_{13})\theta_{NO}\theta_N \tag{32}$$

Then, Eq. (33) can be obtained after resolution and rearrangement.

$$\frac{\theta_N}{\theta_{NO}} = \frac{(k_{12}+k_{13})}{4k_{11}}\left(\sqrt{1+\frac{8k_{11}k_{10}\sqrt{K_H P_{H_2}}}{(k_{12}+k_{13})^2 K_{NO}P_{NO}}} - 1\right) \tag{33}$$

Subsequent substitution of Eq. (33) in Eq. (31) leads to Eq. (34).

$$\frac{4r_{N_2}}{r_{N_2O}} + 1 = \frac{(k_{12}+k_{13})}{k_{11}}\left(\sqrt{1+\frac{8k_{11}k_{10}\sqrt{K_H P_{H_2}}}{(k_{12}+k_{13})^2 K_{NO}P_{NO}}} + \frac{3k_{12}}{k_{13}}\right) \tag{34}$$

The weak partial pressure dependency of the N_2O-selectivity earlier observed on Rh based catalysts for the NO/CO reaction [40] has been related to a very small value for the ratio $8k_{11}k_{10}\sqrt{K_H P_{H_2}}/(k_{12}+k_{13})^2 K_{NO}P_{NO}$. Such a condition is fulfilled if the numerical values for K_{NO}, k_{12} and k_{13} are significantly higher than the calculated values of K_H, k_{11} and k_{10}. In that case Eq. (33) can be simplified leading to Eq. (33) which demonstrates that the selectivity is independent of the partial pressure of NO.

$$\frac{r_{N_2}}{r_{N_2O}} \cong \frac{k_{12}}{k_{13}} \tag{37}$$

In this present study, Fig. 4 shows that the relative rate r_{N_2}/r_{N_2O} remains unchanged on $0.18Rh/Al_2O_3$ within the margin of error corresponding to $k_{12}/k_{13} \cong 3.5$. Such a result is consistent with a very low relative concentration of N_{ads} in comparison with NO_{ads}. Hence, the recombination of two chemisorbed N atoms (step 11) is expected to be much slower than steps (12) and (13) leading to the conclusion that the production of N_2 on $0.18Rh/Al_2O_3$ would mainly involve step (12). Such a result agrees with theoretical calculations in Table 2 reporting a higher activation barrier for the recombination of two chemisorbed N atoms. Regarding $2.5Pd\text{-}0.18Rh/Al_2O_3$ it is worthwhile to note that this catalyst mimics $0.18Rh/Al_2O_3$ with r_{N_2}/r_{N_2O} insensitive to partial pressure conditions. However, the related value for $k_{12}/k_{13} \cong 1.40\text{–}1.45$ is much lower than that of $0.18Rh/Al_2O_3$. For further comparisons, k_{12}/k_{13} has been tentatively estimated at 40 °C on $0.18Rh/Al_2O_3$ from the slope of the plot $\ln r_{N_2}/r_{N_2O}$ vs. $1/T$ in Fig. 7. The slope is related to the deviation between activation energy E_{12} and E_{13} ascribed to the formation of N_2 and N_2O. The numerical solution allows a rough estimation of k_{12}/k_{13} at 40 °C on $0.18Rh/Al_2O_3$ of approximately ≅7800 which suggests that Rh addition to Pd has a strong detrimental effect on the formation of nitrogen with a significant lower value for k_{12}/k_{13}. Despite electronic effects cannot be strictly ruled due to peculiar interactions between Pd and Rh, it seems obvious that no significant electronic disturbance is discernible from XPS measurements particularly on the Pd 3d core level of *in situ* reduced catalysts that could explain a poorer nitrogen selectivity on $2.5Pd\text{-}0.18Rh/Al_2O_3$. As earlier, discussed, it seems likely that a better selectivity in favour of the NO/H_2 reactions and the predominant production of N_2O on this latter catalyst could be more related structural effects since the adsorptive properties of Rh and the structure-sensitive NO dissociation will govern the concentration of chemisorbed N_{ads} and the subsequent selectivity towards the production of N_2 or N_2O.

5. Conclusion

The kinetics of the NO/H_2 reaction has been extensively investigated on freshly-prepared monometallic and bimetallic Pd and Rh based catalysts in order to evaluate precisely the real impact of Rh on the adsorptive properties of Pd and on the reactivity of intermediates in the presence of oxygen but near stoichiometric conditions. Rate measurements showed that Rh is significantly less active when H_2 is used as reducing agent but much more selective because the NO/H_2 reaction occurs more readily on Rh than the H_2/O_2 reaction while the opposite trend characterizes Pd. It is also obvious that the production of nitrogen occurs more extensively

on 0.18Rh/Al_2O_3 than on 2.5Pd/Al_2O_3. Regarding the impact of Rh incorporation to Pd on the kinetic behaviour, unexpected trends were observed due to the involvement of none competitive adsorptions of NO on rhodium whereas H_2 and O_2 would preferentially adsorb on Pt. This hypothesis seems to correctly fit rate measurements and the selectivity to N_2O production which mimics that of rhodium with a predominant NO/H_2 reaction at the expense of the H_2/O_2 reaction occurring predominantly on 2.5Pd/Al_2O_3. However, the most important evidence is provided by the insensitivity of the selectivity to N_2O production to partial pressure conditions on 2.5Pd-0.18Rh/Al_2O_3 that emphasizes the fact of none competitive adsorptions with steps for the production of N_2 and N_2O involving only rhodium. This could explain the poorest selectivity towards the production of nitrogen when Rh is added to Pd. In conclusion all these information provide guidelines of practical interest showing that Rh and Pd must be segregated on different support materials for obtaining a cooperative effect in NGV catalysts.

Acknowledgements

The authors would like to thank, the French Agency of Energy and Environment (Ademe) and the North Region through the Institut de Recherche en Environnement Industriel (IRENI) for a fellowship (Y. Renème), Umicore Company which supplied model NGV catalyst samples. Finally, we would like to thank Arnaud Beaurain and Martine Trentesaux who conducted XPS measurements.

References

[1] W.C. Hecker, A.T. Bell, J. Catal. 92 (1985) 247.
[2] M. Shelef, G.W. Graham, Catal. Rev. Sci. Eng. 36 (1994) 433.
[3] T.W. Root, L.D. Schmidt, G.B. Fisher, Surf. Sci. 134 (1983) 30.
[4] R.J. Gorte, L.D. Schmidt, J.L. Gland, Surf. Sci. 109 (1990) 367.
[5] D.T. Wickam, B.A. Banse, B.E. Koel, Surf. Sci. 243 (1991) 83.
[6] F. Zaera, C.S. Gopinath, Chem. Phys. Lett. 332 (2000) 209.
[7] F. Zaear, C.S. Gopinath, J. Chem. Phys. 116 (2002) 1128.
[8] B. Frank, G. Emig, A. Renken, Appl. Catal. B 19 (1998) 45.
[9] R. Burch, M.D. Coleman, J. Catal. 208 (2002) 435.
[10] F. Dhainaut, S. Pietrzyk, P. Granger, Langmuir 25 (2009) 13673.
[11] F. Dhainaut, S. Pietrzik, P. Granger, J. Catal. 258 (2008) 296.
[12] H. Permana, K.Y.S. Ng, C.H.F. Peden, S.J. Schmieg, D.K. Lambert, D.N. Belton, J. Catal. 164 (1996) 194.
[13] R.M. Wolf, J.W. Bakker, B.E. Nieuwenhuys, Surf. Sci. 246 (1991) 135.
[14] P. Granger, P. Malfoy, L. Leclercq, G. Leclercq, J. Catal. 223 (2004) 142.
[15] M. Salaün, A. Kouakou, S. Da Costa, P. Da Costa, Appl. Catal. B 88 (2009) 386.
[16] F. Klingstedt, A.K. Neyestanaki, R. Byggningsbacka, L.-E. Lindfors, M. Lundén, M. Petersson, P. Tengström, T. Ollonqvist, J. Väyrynen, Appl. Catal. A 209 (2001) 301.
[17] I. Nova, L. Lietti, L. Castoldi, E. Tronconi, J. Catal. 239 (2006) 244.
[18] W. Epling, J. Parks, G. Campbell, A. Yezerets, N. Currier, N. Campbell, Catal. Today 96 (2004) 21.
[19] A. Ueda, T. Nakato, M. Azuma, T. Kobayashi, Catal. Today 45 (1998) 135.
[20] C.N. Costa, A.M. Efstathiou, J. Phys. Chem. B 108 (2004) 2620.
[21] C.N. Costa, A.M. Efstathiou, J. Phys. Chem. C 111 (2007) 3010.
[22] M. Uenishi, M. Tanigushi, H. Tanaka, Appl. Catal. B 57 (2007) 267.
[23] D.A. Shirley, Phys. Rev. B5 (1972) 4709.
[24] A.S. Mamede, G. Leclercq, E. Payen, P. Granger, L. Gengembre, J. Grimblot, Surf. Interface Anal. 34 (2002) 105.
[25] P. Granger, C. Dathy, J.J. Lecomte, L. Leclercq, M. Prigent, G. Mabilon, G. Leclercq, J. Catal. 173 (1998) 304.
[26] P. Trambouze, H. Van Landeghem, J.P. Wauquier, Les réacteurs chimiques, Conception, Calcul, Mise en Œuvre, Technip, Paris, 1984.
[27] J.F. Lepage, J. Cosyns, P. Courty, E. Freund, J.P. Franck, Y. Yacquin, B. Juquin, C. Marsilly, G. Martino, J. Miquel, R. Montarnal, A. Sugier, H. Van Landeghem, Catalyse de Contact, Technip, Paris, 1978, p. 53.
[28] C.M. Mendez, H. Olivero, D.E. Damiani, M.A. Volpe, Appl. Catal. B 84 (2008) 156.
[29] J.M. Padilla, G. Del Angel, J. Navarrette, Catal. Today 133–135 (2008) 541.
[30] A. Suopanki, R. Polvinen, M. Valden, M. Häkönen, Catal. Today 100 (2005) 327.
[31] D. Briggs, M.P. Seah, Practical Surface Analysis, vol. 1, 2nd ed., John Wiley, Chichester, 1999, p. 599.
[32] A. Talo, J. Lathinen, P. Hautojärvi, Appl. Catal. B 5 (1995) 221.
[33] D.D. Beck, C.J. Carr, J. Catal. 144 (1993) 296.
[34] R.N. Lamb, B. Ngamsom, D.L. Trimm, B. Gong, P.L. Silveston, P. Praserthdam, Appl. Catal. A 268 (2004) 43.
[35] E. Shustorovich, H. Sellers, Surf. Sci. Rep. 31 (1998) 1.
[36] E. Shustorovich, A.T. Bell, Surf. Sci. 289 (1993) 127.
[37] E. Shustorovich, A.T. Bell, Surf. Sci. 253 (1991) 388.
[38] F. Dhainaut, S. Pietrzyk, P. Granger, J. Catal. 258 (2008) 296.
[39] J. Nováková, Appl. Catal. B 30 (2001) 445.
[40] P. Granger, J.J. Lecomte, C. Dathy, L. Leclercq, G. Leclercq, J. Catal. 175 (1998) 194.
[41] H. Okuyama, W. Siga, N. Takagi, M. Nishima, T. Aruga, Surf. Sci. 401 (1998) 344.
[42] L. Piccolo, A. Piednoir, J.C. Bertolini, Surf. Sci. 600 (2006) 4211.
[43] W.F. Banholzer, Y.O. Park, K.M. Mark, R.L. Masel, Surf. Sci. 128 (1983) 176.
[44] Z. Hu, F.M. Hallen, C.Z. Wan, R.M. Heck, J.J. Steger, R.E. Lakis, C.E. Lyman, J. Catal. 174 (1998) 13.
[45] K.Y.S. Ng, D.N. Belton, S.J. Schmieg, G.B. Fischer, J. Catal. 146 (1994) 394.